

# Titania Polymorphs by Soft Chemistry: Is There a Common Structural Pattern?

Milen Gateshki,<sup>†</sup> Shu Yin,<sup>‡</sup> Yang Ren,<sup>§</sup> and Valeri Petkov<sup>\*,†</sup>

Department of Physics, Central Michigan University, Mt. Pleasant, Michigan 48859, Institute of Multidisciplinary Research for Advanced Materials, Tohoku University, Sendai, 980-8577, Japan, and Advanced Photon Source, Argonne National Laboratory, Argonne, Illinois 60439

Received December 22, 2006. Revised Manuscript Received March 6, 2007

The structural aspects of a soft chemical route<sup>1</sup> employed to obtain nitrogen-doped brookite, rutile, or anatase fine crystallite powders are revealed by total X-ray diffraction and atomic pair distribution function analysis. It is found that the route first passes through a heavily disordered phase consisting of nanosize layers of TiO<sub>6</sub> octahedra, similar to those occurring in the lepidocrocite-type structure. That phase is then transformed into a particular titania polymorph by rearranging the layers in a controlled way. The lepidocrocite-type structure thus again proves to be a very useful template in the soft chemistry of titania.

## Introduction

Titania, TiO<sub>2</sub>, is used in a number of important technological applications such as functional ceramics, reinforced polymers, pigments, photocatalysts, gas sensors, solar energy conversion, and Li-ion batteries.<sup>2</sup> It occurs in three crystalline polymorphs: rutile, anatase, and brookite. All are built of Ti–O<sub>6</sub> octahedra; the way the octahedra couple to each other into a 3D network is slightly different in the different polymorphs. Bulk rutile is the most thermodynamically stable polymorph of titania, and an irreversible phase transition from brookite to anatase and then to rutile usually occurs with increasing temperature. The thermodynamic stability of titania polymorphs, however, also depends on the crystallite size, and because most applications require fine titania powders, it is actually the anatase polymorph that is most frequently used. Anatase, however, exhibits a relatively large band gap (~3 eV), which is unfavorable to some applications such as photocatalysis. This has inspired an intensive search for fine crystallite titania powders with a narrower band gap. A possibility is to switch to the brookite polymorph, which shows an intrinsically narrower band gap (~2 eV<sup>3</sup>). Another, to dope titania with nitrogen, carbon, or fluorine, which too results in a considerable narrowing of the band gap.<sup>4</sup> Recently Yin et al.<sup>1</sup> demonstrated that nitrogen-doped fine crystallite titania powders, with an excellent photocatalytic activity under the irradiation of visible light, can be prepared by a homogeneous precipitation-solvothermal process. As expected, the powders were found to exhibit photocatalytic activity in the sequence of pure brookite > mixture of rutile

and brookite/anatase > pure rutile. The finest crystallite size powders that were produced, however, turned out to be mostly anatase. Further progress may be achieved by increasing the yield of brookite polymorph. This, in turn, requires good knowledge about the structural evolution accompanying the preparation route. Previous studies<sup>1</sup> have shown that it first passes through a heavily disordered phase, formed during the homogeneous precipitation stage, which is then transformed into a particular titania polymorph during the solvothermal stage. Although the structure type of the final product of the process is relatively easy to identify, that of the intermediate one is not, leaving open the question of what indeed is the intermediate (hereafter called precursor) phase from which all three titania polymorphs may be obtained. The problem stems from the fact that the atomic arrangement in heavily disordered materials is difficult to study by traditional techniques for structure determination such as Bragg X-ray diffraction (XRD). Here, we apply total XRD coupled to atomic pair distribution function (PDF) analysis to determine the atomic-scale structure of that precursor phase. We find that it consists of fragmented layers of Ti–O<sub>6</sub> octahedra which, when assembled accordingly, may couple into a fully connected network of either rutile, anatase, or brookite type.

## Experimental Section

**Sample Preparation.** TiCl<sub>3</sub> (Kanto Chem. Co. Inc., Japan) and hexamethylenetetramine (HMT, C<sub>6</sub>H<sub>12</sub>N<sub>4</sub>, Kanto Chem. Co. Inc., Japan) were used as starting materials. A suitable amount of HMT and 21.5 cm<sup>3</sup> of 20 wt % TiCl<sub>3</sub> solution were mixed with 25 cm<sup>3</sup> of distilled water or pure alcohols such as methanol and ethanol. The mixture was placed into a SUS 314 stainless steel autoclave attached to a Teflon tube with an internal volume of 200 cm<sup>3</sup>. The autoclave chamber was flushed with nitrogen gas three times while being heated at 90 °C for 1 h until a highly disordered (precursor) phase precipitated. It was further heated to 190 °C for 2 h, and the pH value of the solution was adjusted to 1, 7, or 9 using 2, 6, or 10 g of HMT, respectively. The solid fraction of the solution was extracted by centrifugation, washed with distilled water and acetone three times, and dried at 80 °C overnight in a vacuum. As a result,

\* Corresponding author. E-mail: petkov@phy.cmich.edu.

<sup>†</sup> Central Michigan University.

<sup>‡</sup> Tohoku University.

<sup>§</sup> Argonne National Laboratory.

(1) Yin, S.; Aita, Y.; Komatsu, M.; Wang, J.; Tang, Q.; Sato, T. *J. Mater. Chem.* **2005**, *15*, 674.

(2) Zhu, H. Y.; Lan, Y.; Gao, X. P.; Ringer, S. P.; Zheng, Z. F.; Song, D. Y.; Zhao, J. C. *J. Am. Chem. Soc.* **2005**, *127*, 6730.

(3) Posternak, M.; Baldereschi, A. *Phys. Rev. B* **2006**, *74*, 125113.

(4) Asahi, R.; Morikawa, T.; Ohwaki, T.; Aoki, K.; Taga, Y. *Science* **2001**, *293*, 269.

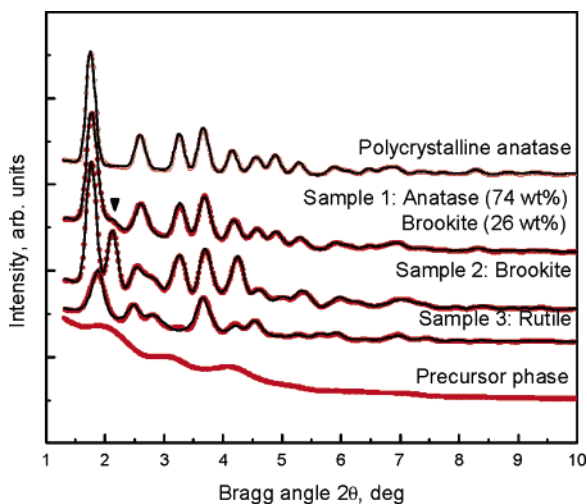


**Figure 1.** XRD patterns for polycrystalline anatase (standard), nitrogen-doped fine titania powders, and the intermediate, highly disordered (precursor) phase. Calculated XRD patterns obtained through Rietveld analyses are shown as lines (in red). A weak diffraction feature coming from the presence of a minor second phase in sample 1 is marked with a triangle (▼).

nitrogen-doped quite fine crystallite ( $\sim 10$ – $20$  nm) titania powders with the anatase (at pH 9 in methanol; hereafter called sample 1), brookite (at pH 1 in water; hereafter called sample 2), or rutile-type (at pH 9 in water; hereafter called sample 3) structure were obtained. More details of the preparation procedure can be found in the literature.<sup>1</sup>

**XRD Experiments.** The precursor phase and the fine crystallite titania powders obtained from it were subject to XRD experiments at the beamline 11-ID-C (Advanced Photon Source, Argonne National Laboratory) using synchrotron radiation of energy 115.227 keV ( $\lambda = 0.1076$  Å). Polycrystalline anatase (from Sigma; average crystallite size of  $\sim 100$  nm) was also measured and used as a reference material. Synchrotron radiation X-rays were employed for two reasons: First, the high flux of synchrotron radiation X-rays allowed us to measure the rather diffuse XRD pattern of the precursor phase with a very good statistical accuracy for a relatively short data collection time. Second, the high energy of synchrotron radiation X-rays allowed us to collect data over a wide range ( $1$ – $30$  Å<sup>-1</sup>) of scattering vectors  $Q$ , which is important<sup>5,6</sup> for the success of the atomic PDF analysis employed here. All samples were sealed between Capton foils and the measurements performed in transmission geometry. Scattered radiation was collected with an imaging plate detector (mar345). Up to 10 images/scans were taken for each of the samples. The corresponding images/scans were combined, subjected to geometrical corrections, integrated and reduced to one-dimensional XRD patterns shown in Figure 1.

## Results

**Traditional Analysis.** As can be seen in Figure 1, the XRD patterns of the anatase standard and nitrogen-doped titania powders show well-defined Bragg peaks, as might be expected for well-ordered materials. Such patterns lend themselves to traditional crystallographic analysis. The analysis was done employing the Rietveld method<sup>7,8</sup> with the help of the program FullProf.<sup>9</sup> The XRD pattern of the standard sample was very well reproduced by a model based

on the anatase structure, shown in Figure 2a. Sample 1 turned out to be a mixture of dominant (74 wt %) anatase and minor (26 wt %) brookite-type phases. The XRD pattern of sample 2 was well-reproduced by a model based on the brookite structure, shown in Figure 2b. That of sample 3 was well-reproduced by a model based on the rutile structure, shown in Figure 2c. In-house XRD experiments on the same samples yielded similar results. Structure parameters resulted from the Rietveld analyses are summarized in Table 1.

**Atomic PDF Analysis. Essentials.** The XRD pattern for the precursor phase, however, is very diffuse in nature (see Figure 1) and could not be analyzed in the traditional way. That is why it was considered in terms of the corresponding atomic PDF, an approach that has recently proven to be very successful in structure studies of heavily disordered oxide materials.<sup>10–13</sup> Because the approach is not so widely recognized and routinely used, as it could be, here we again describe its basic features, in brief. The frequently used reduced atomic PDF,  $G(r)$ , is defined as

$$G(r) = 4\pi r[\rho(r) - \rho_0] \quad (1)$$

where  $\rho(r)$  and  $\rho_0$  are the local and average atomic number densities, respectively, and  $r$  is the radial distance.<sup>5,6</sup> As defined, the PDF  $G(r)$  is a one-dimensional function that oscillates around zero and shows positive peaks at distances separating pairs of atoms, i.e., where the local atomic density exceeds the average one. The PDF  $G(r)$  is a sine–Fourier transform of the experimentally observable reduced structure function

$$F(Q) = Q[S(Q) - 1], \text{ i.e.}$$

$$G(r) = (2/\pi) \int_{Q=0}^{Q_{\max}} F(Q) \sin(Qr) dQ \quad (2)$$

where  $Q$  is the magnitude of the scattering vector  $Q = 4\pi(\sin \theta)/\lambda$ ,  $2\theta$  is the angle between the incoming and outgoing X-rays, and  $\lambda$  is the wavelength of the X-rays used. The structure function  $S(Q)$  is related to the coherent part of the total XRD pattern as follows

$$S(Q) = 1 + [I^{\text{coh}}(Q) - \sum_i c_i |f_i(Q)|^2] / \sum_i c_i f_i(Q)^2 \quad (3)$$

where  $I^{\text{coh}}(Q)$  is the coherent scattering intensity per atom in electron units and  $c_i$  and  $f_i$  are the atomic concentration and X-ray scattering factor, respectively, for the atomic species of type  $i$ . As can be seen from eqs 1–3, the PDF is basically another representation of the XRD data. Exploring the XRD data in real space is, however, very advantageous in case of heavily disordered materials. First, the PDF takes into account all components of the XRD pattern (i.e., the

(7) Rietveld, H. M. *J. Appl. Crystallogr.* **1969**, *2*, 65.

(8) Young, R. A. Ed. *The Rietveld Method*; Oxford University Press: New York, 1996.

(9) Rodríguez-Carvajal, J. *Physica B* **1993**, *192*, 55.

(10) Petkov, V.; Gateshki, M.; Choi, J.; Gillan, E. G.; Ren, Y. *J. Mater. Chem.* **2005**, *15*, 4654.

(11) Gateshki, M.; Hwang, S.-J.; Park, D. H.; Ren, Y.; Petkov, V. *J. Phys. Chem. B* **2004**, *108*, 14956.

(12) Petkov, V.; Gateshki, M.; Niederberger, M.; Ren, Y. *Chem. Mater.* **2006**, *18*, 814.

(13) Mamontov, E.; Brezny, R.; Koranne, M.; Egami, T. *J. Phys. Chem. B* **2003**, *107*, 13007.

(5) Klug, H. P.; Alexander, L. E. *X-ray Diffraction Procedures for Polycrystalline Materials*; Wiley: New York, 1974.

(6) Egami, T.; Billinge, S. J. L. *Underneath the Bragg Peaks. Structural Analysis of Complex Materials*; Pergamon: Oxford, U.K., 2003.

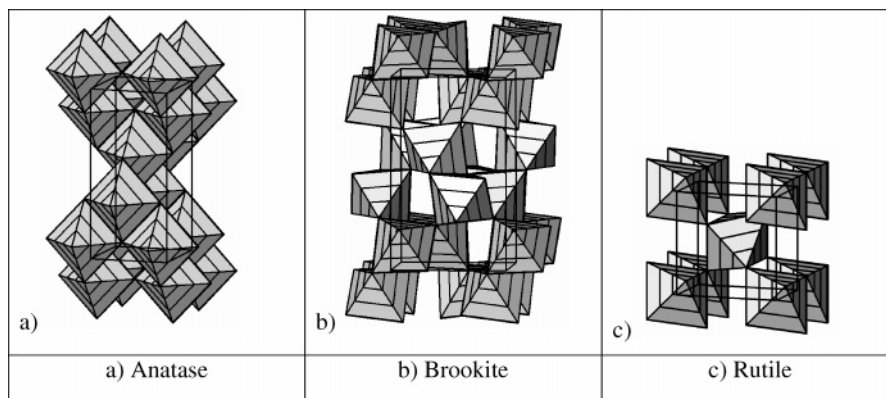


**Figure 2.** Fragments from the crystal structures of (a) anatase, (b) brookite, and (c) rutile representing slightly different 3D networks of TiO<sub>6</sub> octahedra. The corresponding unit cells are outlined with thin solid lines.

**Table 1. Parameters of the Crystalline Lattices of Three Nitrogen-Doped Fine Titania Powders and Polycrystalline Anatase (standard) as Obtained through PDF and Rietveld Analyses<sup>a</sup>**

	crystalline anatase	sample 1: anatase	sample 2: brookite	sample 3: rutile
		PDF Analysis		
<i>a</i> (Å)	3.779(1)	3.782(1)	9.193(3)	4.600(1)
<i>b</i> (Å)	9.494(2)	9.457(4)	5.451(2)	2.956(1)
<i>c</i> (Å)			5.146(2)	
		Rietveld Analysis		
<i>a</i> (Å)	3.784(1)	3.789(3)	9.226(4)	4.626(4)
<i>b</i> (Å)	9.516(2)	9.473(8)	5.466(2)	2.935(4)
<i>c</i> (Å)			5.156(2)	

<sup>a</sup> The crystallographic symmetry of the corresponding lattices is as follows: anatase, *I*<sub>4</sub>*1*/*amd*; brookite, *Pbca*; rutile, *P*<sub>4</sub>*2*/*mmm*. The small differences between the structure parameters resulting from the Rietveld and PDF analyses are due the XRD and PDF not being the same experimental quantity, with the latter being more sensitive to the local atomic ordering than the former.

so-called total XRD pattern), including both the sharper (Bragg-like) and diffuselike components. Thus, both the extended (reflected by the Bragg-like scattering) and local (reflected by the diffuse-like scattering) structural features of the material under study are reflected in an experimental PDF. Here, it is worth noting that the PDF for a material composed of well-defined structural units that are, however, weakly bonded/correlated with respect to each other will have two distinct components – one, well-defined, reflecting the atomic order within the well-defined structural units, and another, not so well-defined, – reflecting the correlations between the atoms from neighboring units.<sup>14,15</sup> Second, thanks to the properties of Fourier transformation the slow oscillating (diffuse-like scattering) components of the total XRD data appear as sharp and, hence, easily identified PDF features in real space. Third, the use of high-energy X-rays allows us to access high values of *Q* (i.e., high-order Fourier coefficients) and, hence, reveal fine structure features differing by only 0.015 nm.<sup>16,17</sup> And last but not the least, atomic PDFs are extracted from total XRD data already corrected for all experimental artifacts and, hence, directly give relative

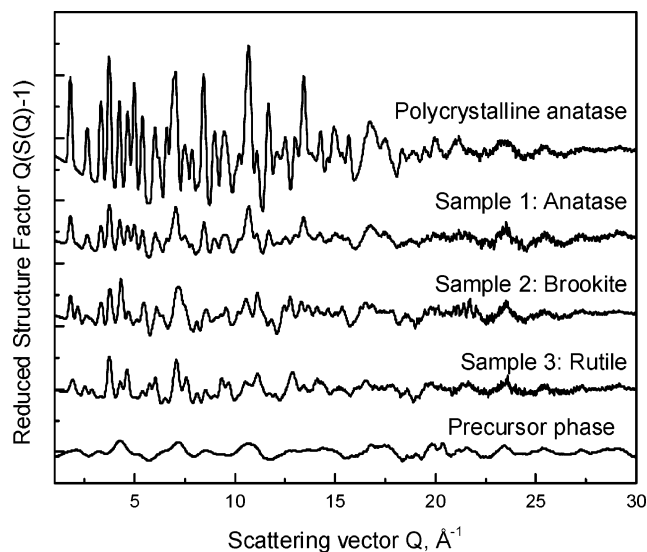


**Figure 3.** Reduced structure factors for polycrystalline anatase (standard), nitrogen-doped fine titania powders, and the precursor phase from which they were obtained.

positions of atoms enabling convenient testing and refinement of structural models.<sup>6,10–14</sup>

**Atomic PDF Analysis: Outcomes and Structure Model Search** Experimental structure factors extracted from the total XRD patterns of polycrystalline anatase (standard), nitrogen-doped fine crystallite titania powders, and the heavily disordered precursor phase are shown in Figure 3. The corresponding atomic PDFs are shown in Figures 4 and 5. The experimental XRD data processing and derivation of atomic PDFs was done with the help of the program RAD.<sup>18</sup>

A comparison between the data of Figure 1 and 3 exemplifies the different way the same diffraction features appear, and hence, are accounted for in structure studies relying on usual powder XRD patterns and the corresponding Structure Factors/PDFs. Usual XRD patterns are dominated by strong diffraction features at lower Bragg angles (wave vectors) and, hence, are mostly sensitive to longer-range atomic ordering. All diffraction features, including those at higher wave vectors, appear equally strong in the corresponding reduced structure factors  $Q[S(Q)-1]$ . This enhances the sensitivity to local (shorter-range) atomic ordering, rendering the Fourier couple  $Q[S(Q)-1]$ /PDF very

(14) Neder, R.; Korsunskiy, V. J. *Phys. Condens. Matter* **2005**, *17*, S125.

(15) Kodama, K.; Iikubo, S.; Shamoto, S. *Acta Crystallogr., Sect. A* **2006**, *62*, 444.

(16) Petkov, V.; Jeong, I.-K.; Chung, J. S.; Thorpe, M. F.; Kycia, S.; Billinge, S. J. L. *Phys. Rev. Lett.* **1999**, *83*, 4089.

(17) Petkov, V.; Billinge, S. J. L.; Shastri, S. D.; Himmel, B. *Phys. Rev. Lett.* **2000**, *85*, 3436.

(18) Petkov, V. J. *Appl. Crystallogr.* **1989**, *22*, 387.



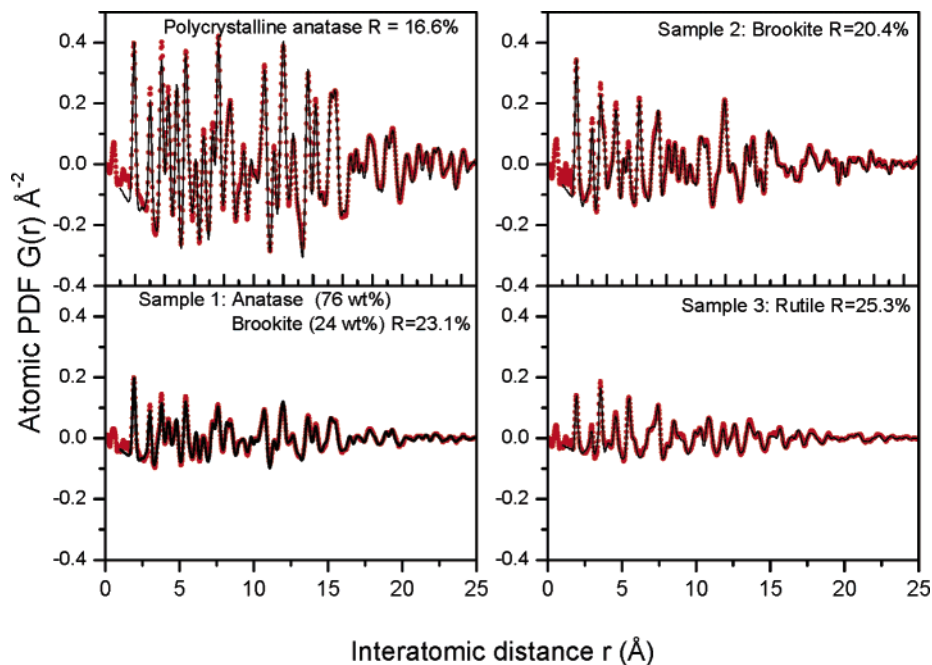


**Figure 4.** Experimental (symbols) and calculated (solid line in red) atomic PDFs for polycrystalline anatase (standard) and nitrogen-doped fine titania powders. The amplitude of the corresponding peaks in the different experimental PDFs are different reflecting the different degree of crystallinity in the studied materials. It is quite high with the standard anatase and, as expected, moderate with the nitrogen-doped fine titania powders. The calculated PDF data are based on the structure types shown in Figure 2.

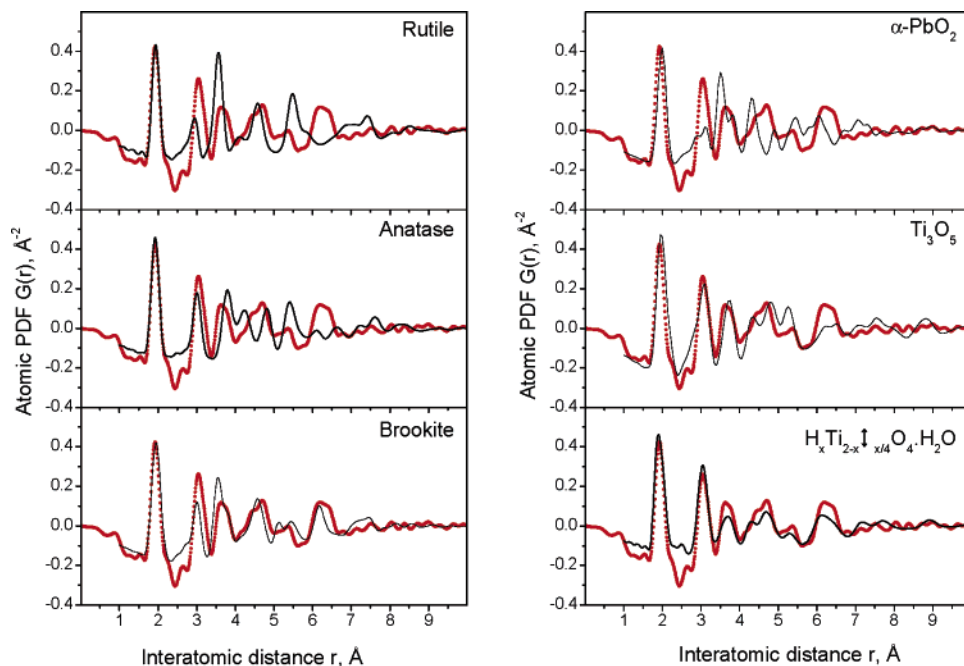


**Figure 5.** Experimental PDF of the precursor phase (symbols) compared with model PDFs (line in red) based on the rutile, anatase, and brookite-type (on the left) and  $\alpha$ - $\text{PbO}_2$ ,  $\text{Ti}_3\text{O}_5$ , and  $\text{H}_x\text{Ti}_{2-x/4}\text{O}_4 \cdot \text{H}_2\text{O}$  (lepidocrocite)-type structures (on the right).

well suited to study materials exhibiting a substantially limited length of structural coherence. That the intermediate titania phase is such a material is clearly seen in Figure 5 showing the experimental PDF decaying to zero already at 1 nm. In contrast, the PDFs for polycrystalline anatase (standard) and nitrogen-doped fine crystallite titania powders persist to much longer interatomic distances, as it should be with materials exhibiting a long-range (i.e., crystalline-type) atomic ordering. As can be seen in Figure 4, the PDFs for the crystalline titania samples are well-reproduced by the structure models already verified by Rietveld analyses. The

PDF calculations were done with the help of the program PDFDFIT.<sup>19</sup> The resulting structure parameters are summarized in Table 1.

As can be seen in the Table, Rietveld (relying only on the Bragg component of the XRD patterns) and PDF (relying on the total XRD patterns) analyses yield very similar results. Rietveld analysis, however, cannot properly handle the very diffuse XRD pattern of the precursor phase. On the other hand, the PDF of the precursor phase shows well-defined

(19) Proffen, Th.; Billinge, S. J. L. *J. Appl. Crystallogr.* **1999**, *32*, 572.

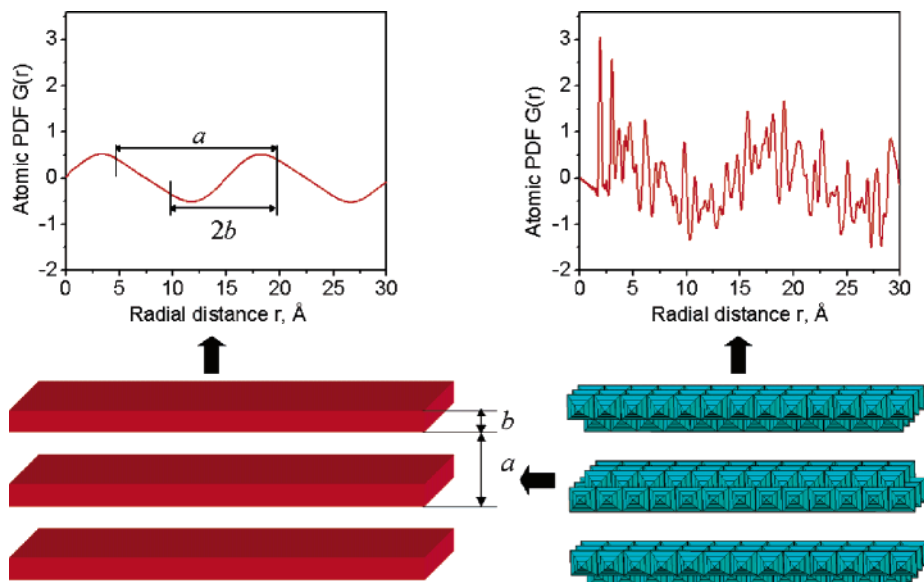


**Figure 6.** Stack of regularly arranged long layers (shown on the left) will produce a slowly varying with  $r$  contribution to the corresponding PDF. The period of this low-frequency PDF oscillation would depend both on the thickness of the layers and the interlayer distance. The well-defined pairs of atoms inside a single layer (i.e., the intralayer atomic correlations) will produce a contribution of much higher frequency. Both contributions (inter and intralayer) will result in a PDF with a characteristic saw shape. The model PDF shown (on the right) has been calculated assuming an “imaginary” stack of long lepidocrocite-type layers, each with thickness  $b = 5$  Å, regularly spaced at a distance  $a = 15$  Å.

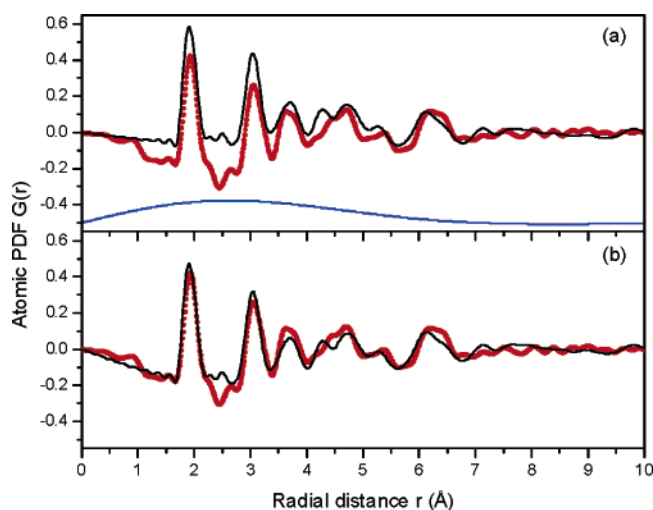


**Figure 7.** (a) Experimental PDF of the precursor phase (symbols) and a model PDF (line in red) corresponding to short ( $\sim 1$  nm) lepidocrocite-type layers regularly spaced at a distance of 14.5 Å. The interlayer contribution to the model PDF is shown in the lower part of the graph (in blue). (b) Calculated PDF reflecting only intralayer atomic pairs/correlations, i.e., corresponding to a model envisioning short, irregularly arranged (piled up) lepidocrocite-type layers.

features allowing an unambiguous structure search and refinement. In particular, the first peak in the PDF of the precursor phase is quite narrow and centered at about 1.9 Å, which is the Ti–O distance in Ti–O<sub>6</sub> octahedra. This observation shows that well-defined Ti–O<sub>6</sub> octahedra are already formed during the homogeneous precipitation stage of the chemical process employed by Yin et al.<sup>1</sup> It prompted us to narrow the search for the precursor phase structure to models built of Ti–O<sub>6</sub> octahedra. No such a useful hint could have resulted from an analysis of the usual XRD pattern alone. Several such models were attempted, including rutile, anatase, brookite, a TiO<sub>2</sub> phase with an  $\alpha$ -PbO<sub>2</sub> type structure observed at pressures higher than 5 GPa,<sup>20</sup> a Ti<sub>3</sub>O<sub>5</sub>-type (monoclinic) structure,<sup>21</sup> titanate with a lepidocrocite-type

structure,<sup>22</sup> H<sub>2</sub>Ti<sub>3</sub>O<sub>7</sub>,<sup>23</sup> TiO<sub>2</sub> with a baddeleyite-type structure observed at pressures above 12 GPa,<sup>20</sup> and Ti<sub>4</sub>O<sub>7</sub>-type structure.<sup>24</sup> Those structures are all built of interconnected TiO<sub>6</sub> octahedra with the number of the neighboring units differing in the different structures. The model PDFs were computed on the basis of literature data (unit-cell constants and atomic positions) for the corresponding structure types, including data for the root-mean square (rms) atomic vibrations at room temperature. The very limited length of structural coherence in the precursor phase was modeled by multiplying the model PDF data with a decaying exponent as has been suggested<sup>25</sup> and implemented<sup>26</sup> in the literature. The effect of the correction is to depress the PDF uniformly without changing its shape. The calculations were again done with the help of the program PDFFIT.<sup>19</sup> Selected results from the model calculations are shown in Figure 5. As can be seen in the figure, the experimental PDF is sensitive enough to discriminate between the different models tested. From all that, one based on the lepidocrocite emerged as the best approximation to the precursor phase structure.

## Discussion

**Structure Model Refinement.** Crystalline lepidocrocite is built of parallel layers of edge-sharing TiO<sub>6</sub> octahedra,<sup>22,27</sup> as shown in Figure 6. As the results of our study suggest, TiO<sub>6</sub> octahedra in the titania precursor phase are coupled in a similar way. The layers of octahedra extend over very

(20) Swami, V.; Kuznetsov, A.; Dubrovinsky, L. S.; McMillan, P. F.; Prakapenka, V. B.; Shen, G.; Muddle, B. C. *Phys. Rev. Lett.* **2006**, *96*, 135702.

(21) Grey, I. E.; Li, C.; Madsen, I. C. *J. Solid State Chem.* **1994**, *113*, 62.  
(22) Sasaki, T.; Watanabe, M.; Michiue, Y.; Komatsu, Y.; Izumi, F.; Takenouchi, T. *Chem. Mater.* **1995**, *7*, 1001.

(23) LeBail, A.; Fourquet, J. L. *Mater. Res. Bull.* **1992**, *27*, 75.

(24) Le Page, Y.; Marezio, M. *J. Solid State Chem.* **1984**, *53*, 13.

(25) Ergun, S.; Schehl, S. R. *Carbon* **1973**, *11*, 127.

(26) Zhang, H.; Gilbert, B.; Huang, N.; Banfield, J. F. *Nature* **2003**, *424*, 1025.

(27) Mao, Y.; Wong, S. S. *J. Am. Chem. Soc.* **2006**, *128*, 8217.

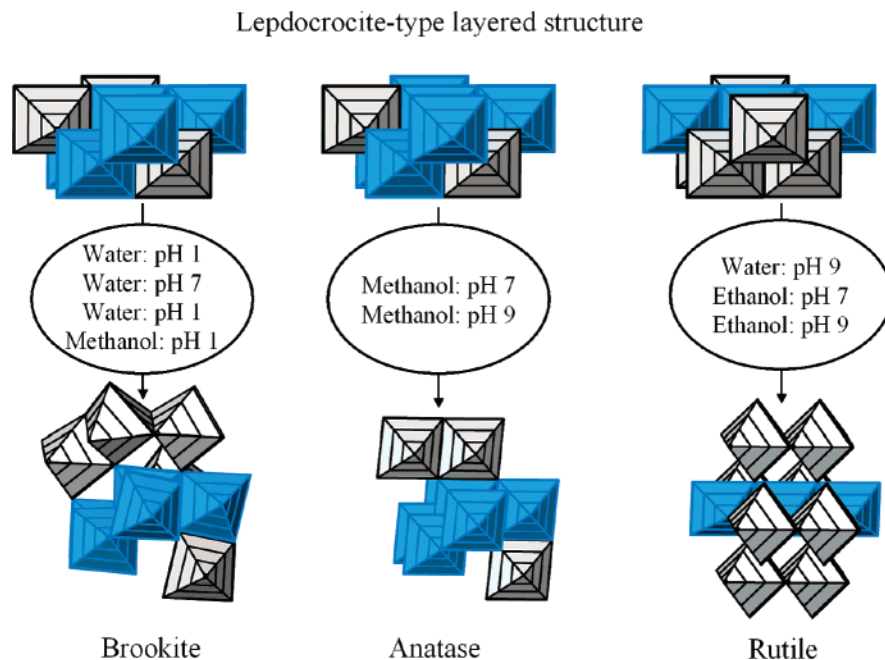


**Figure 8.** Fragments (in different orientations) from the 3D structures of the three stable titania polymorphs (the lower part) and the heavily disordered precursor phase (the upper part) from which they are obtained. As can be seen similar local structural units (shown in blue) occur in the precursor phase and the three crystalline titania polymorphs. This well-explains the marked flexibility of the chemical route of Yin et al.<sup>1</sup> The chemical conditions under which a particular titania polymorph is obtained are shown for each of the cases (in the middle).

long distances in crystalline lepidocrocite (see Figure 6), but are obviously of a very limited length in the precursor phase because the interatomic correlations in it are seen to vanish at distances of approximately 1 nm (see Figure 5). Furthermore, regularly spaced octahedral layers would result in a prominent low-frequency oscillation in the corresponding PDF, as demonstrated in Figure 6. The present experimental PDF data, however, do not show such an oscillation, indicating that the lepidocrocite-type layers in the precursor phase are not regularly stacked either. As a matter of fact, the agreement between the model and experimental PDF is improved when the layer–layer (interlayer) correlation present in the regular (crystalline) lepidocrocite structure is eliminated from the model, as shown in Figure 7. Details of this correction procedure are discussed in the literature.<sup>14,15</sup> Thus, the results of a PDF-guided structure model search and refinement show that the precursor phase we studied is a kind of pile up of quite short layers/fragments of  $\text{TiO}_6$  octahedra coupled according to the scheme observed in lepidocrocite. The lack of an extended structural order in the precursor phase may not come as a surprise considering the very mild conditions (heating at  $\sim 90^\circ\text{C}$ ) under which it is obtained. As we discuss below, it is this lack that indeed allows the precursor to evolve into any of the crystalline (3D ordered) titania polymorphs.

**Titania Synthesis: Implications.** Titanates with layered structure have been found to be very good precursor phases for the preparation of fine crystallite rutile and anatase<sup>2,27,28</sup> at mild conditions (i.e., through a low-temperature synthesis). Recent studies of Tomita et al.<sup>29</sup> find that brookite too can be prepared through a soft chemistry route involving an

intermediate phase of chains of  $\text{TiO}_6$  octahedra. Also, it has long been recognized that low-temperature synthetic routes benefit when passed through a stage involving an intermediate (precursor) phase having common structural features (building blocks) with the targeted product.<sup>2</sup> These already known facts and the new structural knowledge obtained here may explain the marked flexibility of the soft chemical route of Yin et al.<sup>1</sup> as follows: As can be seen in Figure 8, a common structural feature of layered lepidocrocite and 3D network-type anatase, rutile, and brookite is the presence of a characteristic unit of a few (4–6, as explained in the literature<sup>29</sup>) edge-sharing octahedra. Thus, through a relatively small rearrangement of the structural units within the short (nanosize) lepidocrocite-type layers and a controlled stacking (involving direct assembly and/or shear<sup>29</sup>) of those layers into a 3D network, the precursor phase may be, and as a matter of fact is, converted into any of the three crystalline polymorphs of titania. As demonstrated by Yin et al.,<sup>1</sup> the way the layers/fragments of  $\text{TiO}_6$  octahedra in the precursor rearrange may be controlled is by selecting the solvent and acidity (pH) at which the solvothermal treatment is done. This structural mechanism also well-explains why crystalline rutile produced by the present chemical route is less perfect than the brookite and anatase fine powders, as observed in the literature.<sup>1</sup> This comes from the fact that rutile is less similar to the precursor phase than anatase and brookite (see Figure 5, on the left) and, hence, it needs a higher degree of structural rearrangement to be obtained. This may not be easily achieved at mild chemical conditions/low temperature. Interestingly, the observed structural imperfection of rutile was ascribed to the nitrogen doping in.<sup>1</sup> The present study shows that nitrogen does not have a measurable effect on the atomic-scale structure of any of the fine titania powders doped with it (see the structure parameters reported

(28) Fukuda, K.; Sasaki, T.; Watanabe, M.; Nakai, I.; Inaba, K.; Omote, K. *Cryst. Growth Des.* **2003**, *3*, 281.

(29) Banfield, J.; & Veblen, D. *Am. Mineral.* **1992**, *77*, 545.

in Table 1). What is more important is that the present study suggests a possible way to steer the synthetic route of Yin et al.<sup>1</sup> toward increasing the yield of brookite polymorph while keeping the crystallite size very small. As the results presented in Figure 5 show, the atomic ordering in the precursor phase is closer to brookite (compare the way the corresponding model PDFs approach the experimental data) than to those of rutile and anatase. So if, for example, the second (solvothermal) step of the chemical route is carried out at temperature lower and time shorter than those reported in the literature,<sup>1</sup> not only the formation of anatase and rutile polymorphs but the crystallite growth would be further suppressed, likely resulting in very fine nitrogen-doped titania powders with the structure of brookite only. Here it may be added that layered, lepidocrocite-like fragments have also been used as precursors in other soft chemical processes yielding fine titania powders,<sup>30</sup> nanosheets,<sup>31,32</sup> nanowires,<sup>27</sup> and nanotubes.<sup>33</sup> Thus lepidocrocite emerges as a very useful structural template that may be used to control the outcomes of soft chemistry of fine crystallite and nanostructured titania.

---

(30) Tomita, K.; Petrykin, V.; Kobayashi, M.; Shiro, M.; Yoshimura, M.; Kakihana, M. *Angew. Chem., Int. Ed.* **2006**, *45*, 2378.

(31) Sasaki, T.; Watanabe, M.; Hashizume, H.; Yamada, H.; Nakazawa, H. *J. Am. Chem. Soc.* **1996**, *118*, 8329.

(32) Gateshki, M.; Hwang, S.-J.; Park, D. H.; Ren, Y.; Petkov, V. *Chem. Mater.* **2004**, *16*, 5153.

## Conclusions

Total X-ray diffraction and PDF data analysis can be successfully employed to determine the atomic scale structure of heavily disordered oxides such as the intermediate phase<sup>1</sup> used to obtain nitrogen-doped fine crystallite titania powders. The phase is found to be built of nanosize layers/fragments of TiO<sub>6</sub> octahedra arranged according the coupling scheme found in lepidocrocite. As such, the precursor phase may be converted into any of the titania polymorphs (anatase, brookite, or rutile) in a controlled way. Thus lepidocrocite again proves to be a very useful template in the soft chemistry of titania. Possibilities exist to streamline the conversion process<sup>1</sup> further and increase the yield of the brookite polymorph.

**Acknowledgment.** The work was supported by the NSF through Grant DMR 0304391(NIRT) and CMU through Grant REF C602281. Use of the Advanced Photon Source was supported by the U.S. Department of Energy, Office of Science, Office of Basic Energy Sciences, under Contract DE-AC02-06CH11357.

CM0630587

---

(33) Chen, Q.; Du, G. H.; Zhang, S.; Peng, L.-M. *Acta Crystallogr., Sect. B* **2002**, *B58*, 587.